J Appl Electrochem (2010) 40:311–320
DOI 10.1007/s10800-009-9977-0

ORIGINAL PAPER

Electrochemical evaluation of patinas formed on nineteenth century bronze bells

F. Rodríguez-Acuña · J. Genescá · J. Uruchurtu

Received: 18 January 2009 / Accepted: 17 August 2009 / Published online: 27 August 2009

Abstract The cathedral of Cuernavaca City, Mexico is one of the earliest monuments built in the American Continent by the Spanish Conquerors. The cathedral lodges a collection of historic artifacts including eight bells. The aim of this study was to provide preliminary information for the conservation diagnosis of the historic bells. A set of three bells dating back to the nineteenth century was studied. Two of the bells present a crack and the third and oldest remains complete. Metallurgical characterization and electrochemical evaluation were used to describe the behavior of the patinas formed on the surfaces of the bells. Studies were done "in situ" over the surface of the artifacts. Preliminary experiments were carried out using a modern cast bronze with equivalent chemical composition. Besides the useful information for conservation purposes, the work depicts the behavior of an ancient material exposed to the atmosphere for a long period of time. The obtained data suggest a relationship between alloy composition, especially tin and lead content and electrochemical properties of the materials. Techniques used include potential measurements as function of time, potentiodynamic polarization curves, electrochemical impedance spectroscopy, electrochemical noise as well as metallography.

Keywords Bronze conservation · Bronze corrosion · Patinas assessment · Electrochemical techniques

F. Rodríguez-Acuña (✉) · J. Genescá
Dpto. Ingeniería Metalúrgica, Facultad Química, UNAM,
Ciudad Universitaria, 04510 Mexico, D.F., Mexico
e-mail: faustic@hotmail.com

J. Uruchurtu
Universidad Autónoma del Estado de Morelos-CIICAp,
Av. Universidad 1001, Col. Chamilpa, Cuernavaca,
Morelos, Mexico

1 Introduction

The Mexican Cathedral of Cuernavaca is one of the earliest monuments built by the Spanish Conquerors in the American Continent during the XVI (sixteenth) century. Due to its historic relevance, this monument was declared World Heritage in 1994 by the UNESCO [1]. The collection of historic artifacts and architectonic structures in this cathedral has been enriched since the time of its foundation. A collection of eight bronze bells is located in the single baroque tower of the historic building. The location is presented in Fig. 1.

The historic bells from Cuernavaca represent an important source of aesthetic, musical, and archaeological information [2]. Therefore, their conservation is a priority. The first step in such process was establishing their conservation diagnosis. The aim of this work was to perform an electrochemical evaluation of the patinas from three of the historic bells which date back to the nineteenth century. The obtained information contributed to the conservation diagnosis of the artifacts. From the strict materials science point of view, the novelty of this work consisted of describing materials produced through ancient manufacture technologies, which have been exposed for a long period to atmospheric corrosion.

Only three of the eight bells were studied due to legal restrictions. These bells date back to the nineteenth century, fact revealed by the inscriptions in their surface. The two more recent bells present a crack, possibly caused by corrosion fatigue attack failure over the surface.

The cathedral is located in the city center and in the nineteenth century it was surrounded by cattle and horse stables [3]. Therefore, it is possible that ammonia vapors coming from these sources were available to react with other pollutants to form ammonia compounds responsible

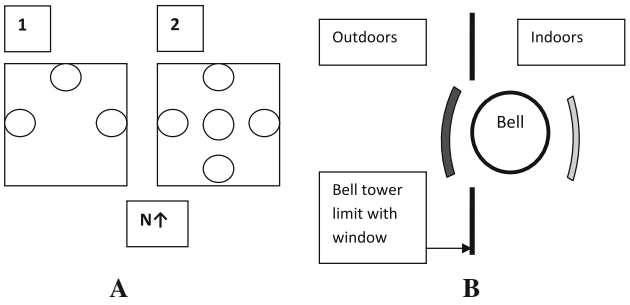

Fig. 1 **a** Position and location of the eight bronze bells in first floor and second floor of the bell tower. **b** Definition of major surfaces in the bells. Exposed surface (*dark gray*), protected surface (*pale gray*) relate to position in reference to the window. Internal surface refers to the inner surface of the body of the bell related to the clapper

for corrosion fatigue cracking in copper and bronze materials.

As said before, sampling of historic artifacts is restrained, therefore, a modern bronze meant to simulate the chemical composition of the ancient bells was used as reference before applying any treatment to the historic materials. Figure 2a shows one of the studied bells, its general profile and its support technique. Figure 2b shows a detail of the crack in a second studied bell. The bodies of the bells show different colors, which suggested different chemical compositions. Three major surfaces were considered for each bell. This way differential exposure to atmospheric pollutants was taken into consideration. Consequently, some procedures took place in modern material while others were carried out "in situ" on the surfaces of the bells.

A main emphasis of this work was the characterization of original patinas present on the bronze surfaces of the bells. Referring to this, it is possible to mention that bronzes are copper alloys that belong to the family of old metals and have a great resistance to atmospheric corrosion. Due to its durability, bronze has been used in artworks such as architectonic elements and sculptures [4]. Bronzes develop patinas with characteristic colors (from pale blue and green to dark brown and black) when they are exposed to the atmospheric action [5]. Such colorations are considered aesthetic and desirable under certain circumstances. Since the formation of the natural patinas takes several years, they constitute indirect clues of the antiquity of the objects, as well as source of archaeological information [6]. The presence and the quality of the patinas on the historic monuments and artifacts are high-priority factors in conservation terms [7].

Fig. 2 **a** Bell in first floor, north side. **b** Fracture of west bell in second floor

Patinas do not reflect current atmospheric composition only. Instead, their composition and properties show an accumulative process of pollutant action in time [8]. Differential exposure to rain water causes significant differences in the patinas. Therefore, composition and morphology of patinas depend on the specific geographic location, climatic conditions, concentration, and aggressiveness of pollutant agents and even on the position of an artifact in the architectonic context. Copper compounds are the basic components of natural patinas in old bronzes [9].

The study of bronze patinas is an important topic within the field of cultural heritage conservation. The conservation theories propose different interpretations about patinas and their suitable management. At the moment, the generalized tendency is to grant special value to patinas because they are considered as part of the history of the monument itself. Besides, the importance of patinas as protective coatings is taken into account. Patinas can only be modified in a monument if there is scientific evidence to support that current state of the patina is causing harm to the integrity of the monument. In any other cases, they should be protected [10].

2 Experimental procedure

2.1 Sampling

Legal restrictions imply that samples from historical artifacts are limited. Only two square coupons (0.5 cm × 0.5 cm × 0.3 cm) were obtained from each bell. These samples were used in metallographic characterization and semi-quantitative chemical analysis of the metallic core. Corrosion products were obtained from each bell by scrapping a 1 cm × 1 cm surface in each area described in them (exposed, protected, and internal).

2.2 Metallurgical and chemical characterization

One coupon from each bell was embedded in modeling matrix (bakelite) and polished up to 600 grit emery paper. Bronze microstructure and chemical composition were

determined using scanning electron microscopy (SEM) with an instrument JEOL 5900-LV. The microanalysis system is an Oxford ISIS model. The second coupon from each bell was analyzed to know the elemental composition by spectrophotometry induced with plasma. The instrument used was a Perkin-Elmer Optima 4300 DV Optical Emission Spectrometer. Corrosion products were analyzed using X-ray diffraction technique to identify the main crystalline components using a SIEMENS D5000 Kα and Cu ($\lambda =$ 1.5406 Å) with Ni filter. Corrosion products were also observed using SEM.

2.3 Modern bronze fabrication (blank)

After analyzing the chemical composition of the archaeological samples, a chemically equivalent modern alloy was created. Average composition of the three bells was calculated. The modern cast bronze simulated the obtained average composition. The actual composition obtained is shown in Table 1. This was also supported by historical sources describing the bell manufacture process during the nineteenth century [11]. These historical sources describe no heat treatments. A similar crystallography to that of the bells was expected to appear in this modern alloy. The cast was made with a gas furnace and "green sand" molds. The cylindrical coupons obtained had a 1.5-cm diameter and 25-cm long.

2.4 Electrochemical techniques

(a) *Rest Potential Test*. This technique was used to determine the time within which the potential becomes stable under steady conditions. 0.01 M sodium borate solution was used as electrolyte throughout all the experiments due to its buffer solution properties and non-aggressiveness [12, 13]. Both, the modern and historical coupons were immersed and measurements were taken during 15 days. The electrochemical cell consisted of the working electrode, a saturated calomel reference electrode, and a platinum wire as counter electrode.

(b) *Potentiodynamic Polarization* (*Polarization Curves*). This technique was used to characterize electrochemical properties of tested materials (modern and historic). The potentiodynamic sweep was from −300 mV below to 1,000 mV above rest potential with a rate of 100 mV min^{-1}.

(c) *Electrochemical Impedance and Electrochemical Noise*. The electrochemical cell (see Fig. 3) over the surface of the bells consisted of a three electrode set similar to the ones used for electrochemical coating evaluation. This was made using two acrylic tubes, 3 cm in diameter, attached to the bell surface (working electrodes) connected through a capillary bridge. The acrylic tubes were filled with the solution. A standard calomel reference electrode and a platinum wire acting as counter electrode completed the set. Electrochemical Impedance Spectroscopy (EIS) measurements were performed in the frequency interval of 0.005–10,000 Hz with an amplitude of 10 mV at the free corrosion potential by using a Gill ACM Instruments.

Electrochemical noise measurements (EN) in both current and voltage were recorded. To accomplish this, an arrangement using a working electrode (bell face), the tip of a platinum wire as counter electrode for current noise measurements, and a calomel reference electrode was used. The electrochemical noise measurements were made recording simultaneously the potential and current fluctuations at a sampling rate of 1 point per second during a 2,048-s period using an Auto-ZRA ACM instrument connected to a personal computer (instrumental noise level below 10 μV, 10 pA). A first order low pass (1 kΩ resistor

Table 1 Chemical composition of bronze bells by spectrophotometry

Element/bell	A	B	C	Average (%)	Cast (%)
Year of casting	1858	1842	1809		
Conservation state	Damaged	Damaged	Undamaged		
Copper	72.5%	74.5%	72.5%	73.2	73.26
Tin	25%	23%	25.5%	24.5	24.57
Lead	2%	2%	1.5%	1.8	1.45
Iron	0.5%	0.5%	0.5%	0.5	0.46

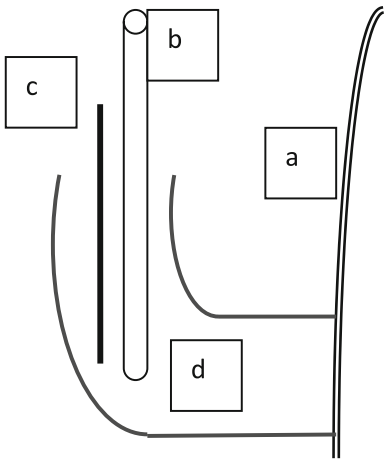

Fig. 3 Electrochemical cell used for 'in situ' measurements. (*a*) Bell surface, (*b*) reference electrode, (*c*) platinum counter electrode, and (*d*) acrylic cell

coupled to 1 μF capacitor) anti-aliasing filter (F) was used ahead of digital data acquisition in order to avoid aliased higher frequency components. The DC trend had to be eliminated in accordance with other investigations because this could originate large distortions in subsequent statistical noise data processing [14]. Therefore, removal of the DC trend from the raw noise data was the first step in the noise analysis. To accomplish this, data processing included trend removal of the signal by first order polynomial fitting and Hanning windowing. Commercial software (origin 5.0) for the polynomial method and Fast Fourier Transform (FFT) algorithm was used to obtain the impedance amplitude spectral density (ASD), in the frequency domain. Both techniques, electrochemical impedance and noise were used "in situ" to avoid additional sampling and damage to the original patinas of the bells. The three described surfaces of the bells were studied.

3 Results and discussion

3.1 Chemical and metallurgical characterization

Table 1 shows the mean composition of the metallic core of the bells obtained by spectrophotometry. Tin and lead were major components of the ancient alloy. This information provided the basis for modern cast bronze formula. The proportions of tin and lead were coherent with the information from historical documents regarding the element percentage which was expected to be around 25% for tin. SEM punctual composition analysis was performed to corroborate chemical composition of the bells. Results are shown in Table 2. Even when some retained phases and inclusions showed slightly higher concentration values for tin or lower values for lead, the average remains within the mean range.

Table 2 Chemical composition of bronzes by SEM

Material	Analyzed points	% Tin	% Lead
Cast bronze	Lamellar (white)	36	1
	Solid solution (gray)	1	1
Bell A	1	25	2
	2	26	2
	3	29	1
	4	–	–
Bell B	1	22	2
	2	25	2
	3	–	–
Bell C	1	26	1
	2	26	1
	3	27	1
	4	–	–

Historical sources describe no heat treatment in the manufacture process of bells. According to the Copper Phase diagram [15], eutectoid structure was expected in the metallography of the bells. Instead, the historic coupons showed a solid solution. The modern alloy showed the expected eutectoid structure. Figure 4 (optical micrograph) and Fig. 5 (SEM micrograph) show the bronze microstructures.

These differences in microstructure may be explained in two ways. The first explanation could be that some details of the bell manufacture process are not fully described in the historical sources. The second possibility is that volume plays a role in the cooling process. Different cooling time ratios may explain the observed differences in microstructure.

Figure 6 presents the patinas of the exposed surfaces of each bell. The blue green color is associated to copper sulfate and copper carbonate commonly present in urban areas. The green colors are observed in these surfaces of the bells which are prone to be in contact with acid rain water. The atmosphere of the city of Cuernavaca is an urban atmosphere calibrated by ISO Standards [16]. This is a relatively recent change due to urban growth. Just a few decades ago it was considered as a rural atmosphere. Therefore, both conditions must be taken into account in the analysis of the bells. The artifacts have been exposed to different conditions for a long period of time. A significant further change relates to the recent activity of Popocatépetl volcano. Figure 7 shows the patinas of the protected surfaces of the bells. Here, we see blue areas as well as black and brown spots. This case is an intermediate situation between the exposed surfaces and the internal surfaces, where yellow and brownish patinas (Fig. 8) associated to basic copper oxides were observed [12].

Table 3 shows the main crystalline compounds, determined by X-ray diffraction, present in the corrosion products from the bell surfaces. Basically, copper oxides prevail in the internal surfaces while mixtures of copper oxides and sulfates are found in the protected surfaces. Copper sulfates were found in the exposed surfaces of Bells B and C while carbonates were found in the exposed surface of Bell A. The presence of specific copper compounds on each kind of surface is easily explained by local environment variations. The exposed surfaces of the bells show higher contents of copper sulfate or calcium carbonate because they are prone to be exposed directly to pollutants and/or acid rain. The corrosion products found in the internal surfaces can be explained as derived only from atmospheric contact. The protected surfaces show an intermediate stage. Dilution of lime stone present in the building materials of the cathedral itself, as well as

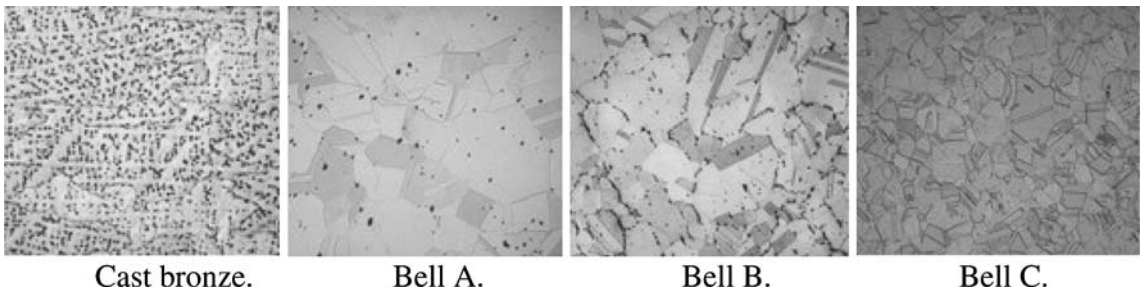

Fig. 4 Bronze microstructures by optical microscope, ×100

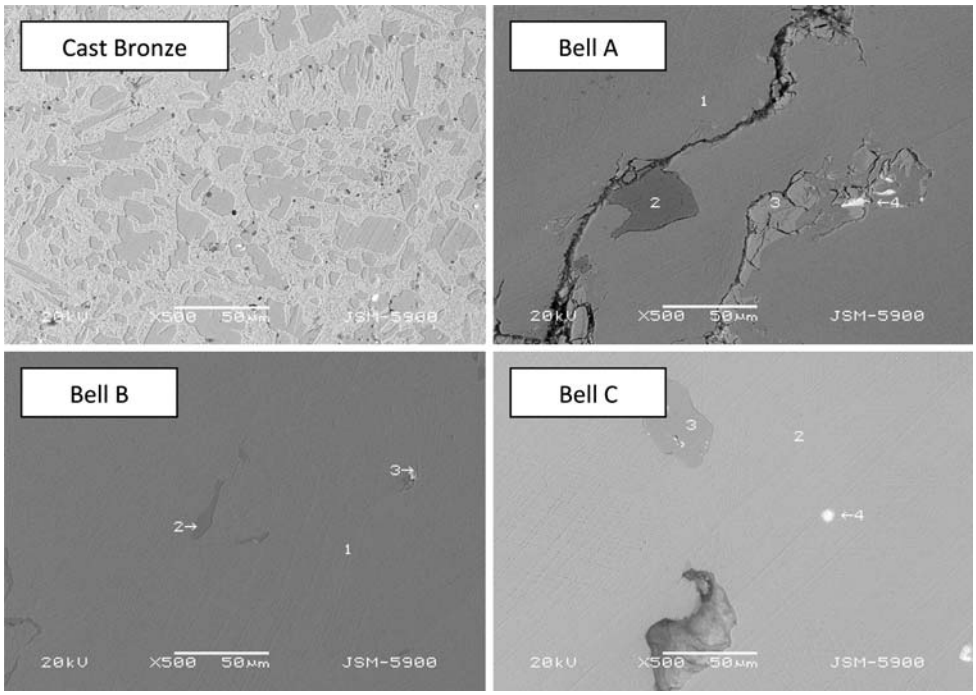

Fig. 5 Bronze microstructures by SEM, ×500

Fig. 6 Patinas on exposed surfaces of bells (area 1 cm^2)

suspended particulate matter, may account for the calcium carbonate found in the corrosion products of Bell A. It is important to state that due to the recent activity of nearby Popocatépetl volcano, sulfur compounds increased in the atmosphere of Cuernavaca. This situation increased the acid rain phenomenon. As additional data, historic documents mention the nearby location of cattle and horses stables. It is a possibility that in the past, nitrogen compounds had a role in the cracking of the bells, apparently caused by corrosion fatigue processes. However, no specific nitrogen compounds were detected in the corrosion products.

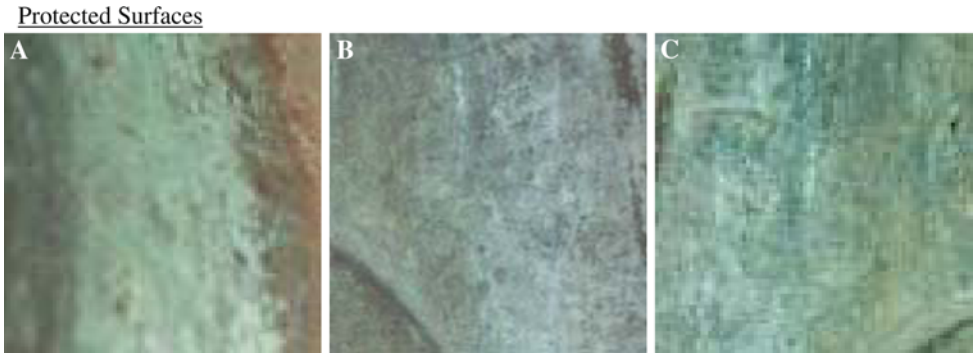

Fig. 7 Patinas on protected surfaces of bells (area 1 cm^2)

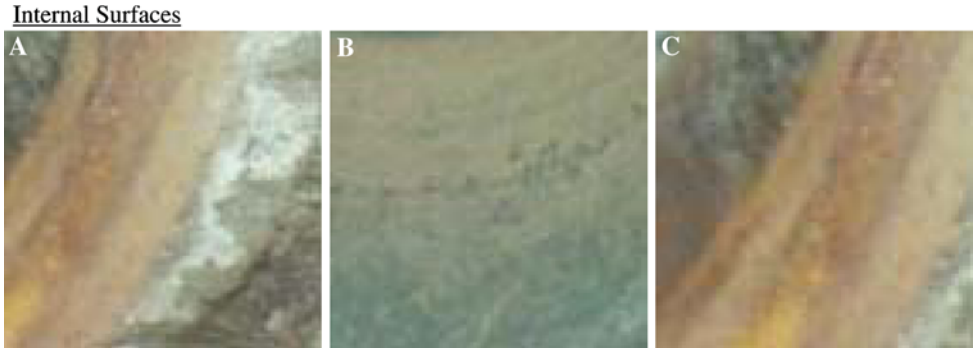

Fig. 8 Patinas on internal surfaces of bells (area 1 cm^2)

Table 3 Corrosion products of bronze bells

Bell	A	B	C
Internal surface	Cu_2O, cuprite	Cu_2O, cuprite	Cu_2O, cuprite
	CuO, tenorite	CuO, tenorite	$CuO{\cdot}3H_2O$
	SiO_2, silica		$CaSO_3{\cdot}4H_2O$
Protected surface	Cu_2O, cuprite	Cu_2O, cuprite	Cu_2O, cuprite
	$CuO{\cdot}3H_2O$	$CuO{\cdot}3H_2O$	$CuSO_4{\cdot}2H_2O$
	$CuSO_4{\cdot}4H_2O$	$CuSO_4$, chalcocyanite	$CaSO_4{\cdot}2H_2O$, gypsum
	$CaSO_3{\cdot}4H_2O$	$CaSO_4{\cdot}2H_2O$, gypsum	$CaSO_3{\cdot}4H_2O$
			SiO_2, silica
Exposed surface	$CuCO_3$	$CuSO_4$, chalcocyanite	Cu_2O, cuprite
	$CaCO_3$, calcite	$CaSO_4{\cdot}2H_2O$, gypsum	$CuSO_4$, chalcocyanite
		SiO_2, silica	

Cuprite (Cu_2O) is a major component of most bronze patinas. This compound was detected in the majority of the bells surfaces. Minerals such as posnjakite ($Cu_4(SO_4)(OH)_6{\cdot}2H_2O$), brochantite ($Cu_4(SO_4)(OH)_6$), malachite ($Cu_2(CO_3)(OH)_2$), atacamite ($Cu_2Cl(OH)_3$), and others have been reported consistently in bronze patinas [17–20]. However, their absence has also been reported in archaeological cases [6]. Some of the compounds found in the corrosion products of the bells are hydrated variations of more common components of bronze patinas. For example, chalcanthite ($CuSO_4{\cdot}5H_2O$) and boothite ($CuSO_4{\cdot}7H_2O$) are more common hydrated sulfates than mineral species $CuSO_4{\cdot}2H_2O$ and $CuSO_4{\cdot}4H_2O$ present in the corrosion products of the bells.

3.2 Electrochemical techniques

Before describing the electrochemical results, it is important to consider the metallographic differences between the blank samples and the metallic core of the bells. The intention of creating the blank samples in conservation studies is to perform preliminary experiments using a sacrificial material instead of risking the limited historic or archaeological materials. Duplication of ancient materials

is not always achieved because ancient manufacture processes are not always comprehended totally. Therefore, the subsequent comparison of electrochemical behavior of modern and historic coupons must be understood as comparison of two materials with similar chemical composition, but different microstructure. Results are reported under this premise.

Figure 9 shows the potential values of bronzes in the 0.1 M sodium borate solution. Free corrosion potential became nobler and stable after 20 h. Bronzes from cracked Bells A and B presented more negative values (−165 and −155 mV SCE, respectively) than the cast modern bronze. Sample from Bell C (non-cracked) presented the most positive value (−125 mV SCE). This initial test suggested that damaged bells behave different compared to the non-cracked one. The open circuit corrosion potential appeared to be directly related to the lead content of the alloy. As the content of lead is higher, the free corrosion potential is more active. The growth of a passive layer over the surface can explain this behavior. The bronzes become nobler and less prone to corrosion as a function of time.

Figure 10 presents the potentiodynamic polarization curves for the bronzes. Bell C shows the more active corrosion potential (−500 mV), while Bell B was the most noble around 50 mV. The corrosion potential observed is directly related to the tin content. As the content of tin increases, the corrosion potential is more active. The pitting potential observed was similar for bronzes A and B (around 1,000 mV) and more negative (500 mV) for bronze C. Once again, this appears to be related to the lead content. The behavior of the passive current may be related with the microstructure differences between the cast bronze and bronzes from the bells. All materials tested present a passive region, bronze Bell A shows a 0.01 mA cm^{-2} passive current while the bronze bell material C presents a lowest peak value around 0.03 mA cm^{-2}. Bronze bell material B shows a 0.1 passive current and the cast bronze material 5 mA/cm^2 passive current, associated to tin content. The passive range appears to be related to the lead content (2% Pb), where the greater range observed was for bronze bell materials A and B (cracked) and the lower to bronze bell material C (1.5% Pb).

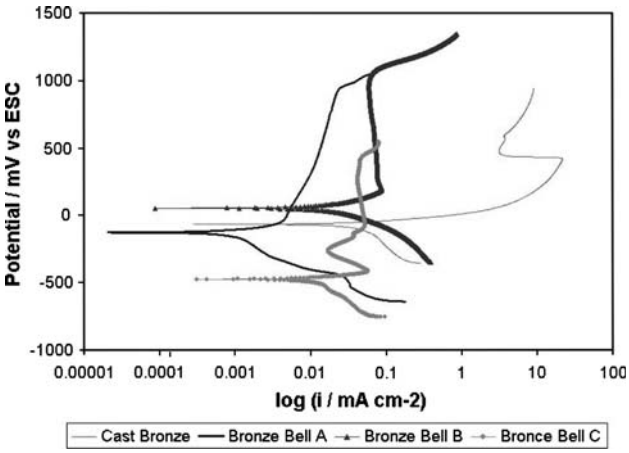

Fig. 10 Potentiodynamic polarization curves for bronze materials

Impedance and electrochemical noise measurements were made 'in situ' over exposed, protected, and internal faces of the different bells. As an example, Fig. 11 presents the impedance Nyquist plots for 'in situ' measurements on the exposed surfaces of the three bells.

The impedance data in the Nyquist plot for the different experiments, shows two depressed, capacitive-like semicircles with their centers in the real axis, one at high frequencies and another one at lower frequencies and sometimes followed by a straight line at the lowest frequencies, indicating a corrosion process under a mixed charge transfer and diffusion control. Diffusion occurs through the protective passive layer [21, 22]. The first semicircle reflects the charge transfer from the metal to the

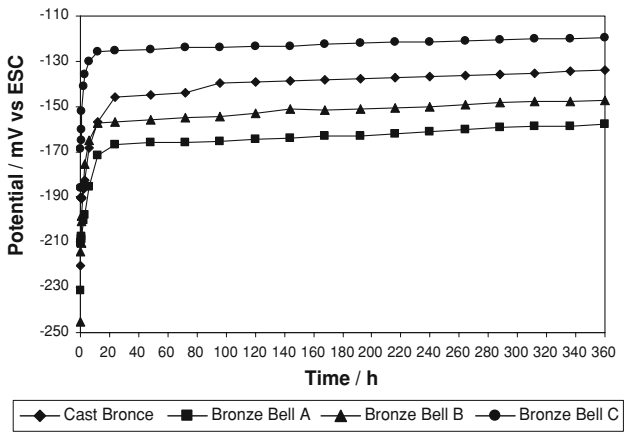

Fig. 9 Free corrosion potential as a function of time for bronze materials

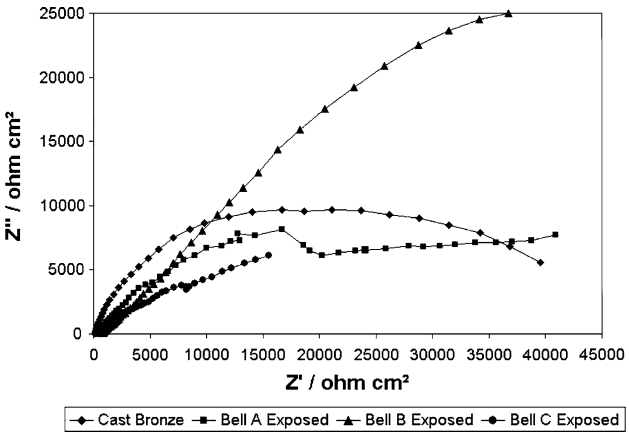

Fig. 11 Nyquist diagram for 'in situ' impedance obtained over bronze bells

electrolyte, while the second one emerges due to adsorption effects and the formation and presence of a protective layer. The semicircle diameter is equivalent to the charge-transfer resistance, R_{ct}, which is inversely proportional to the corrosion current density value, I_{corr}. Thus, the highest R_{ct} value and the lowest the I_{corr} value was for bronze A. The lowest R_{ct} value was for cast bronze. The cast bronze value for charge-transfer resistance is three times higher as shown in Fig. 9, and it is a difference of three orders of magnitude for the passive current. The other semicircle observed belongs to the protective layer or patina formed over the metal surface and this porous resistance value will be related to the protection given by the film (see Fig. 11).

The two depressed semicircle observed in the results obtained, could be described by a complex distribution of the relaxation times or associated time constants. A 45° straight line represents a mass transfer process involving purely ionic diffusion effect. It is considered in this case a diffusion boundary layer to be infinite, i.e., the region of solution near the surface where the concentrations of species are different from the bulk concentration, could be of infinite thickness. The change of the angle degree of the Warburg impedance section (as in our case), folding toward the real axis will mean that at some distance from the surface the concentrations of solution species are constant, due to for example, convection in the solution. This distance is the boundary layer thickness. From the impedance response obtained for the different materials conditions, these different conditions were observed [22] (Table 4).

Figures 12, 13 and 14 present an example of 'in situ' electrochemical potential, current, and noise resistance as a function of time for the different materials tested. The potential and current noise time series showed the typical

Table 4 R_{ct} values obtained by electrochemical impedance technique for each bell surface

Bell	Surface	R_{ct} (Ω)
B (23% Sn)	Exposed	4,550
	Protected	5,200
	Internal	45,900
A (25% Sn)	Exposed	40,937
	Protected	46,667
	Internal	495,000
C (25.5% Sn)	Exposed	36,185
	Protected	44,198
	Internal	777,274

These values were used to calculate corrosion rates

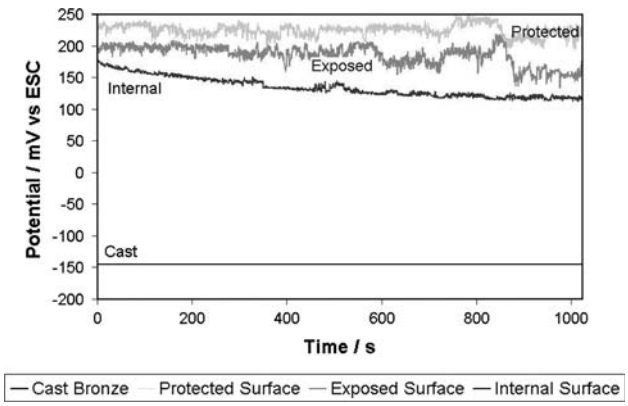

Fig. 12 Time series–potential, Bell C

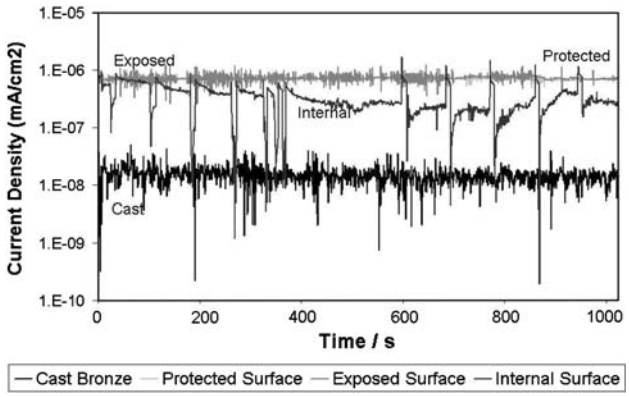

Fig. 13 Time series–current density, Bell C

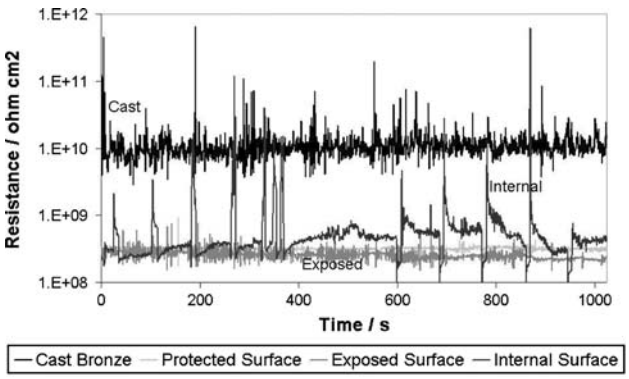

Fig. 14 Time series–resistance, Bell C

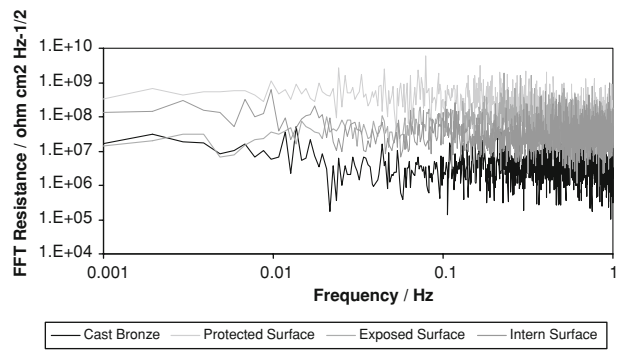

Fig. 15 Resistance noise spectra, Bell C

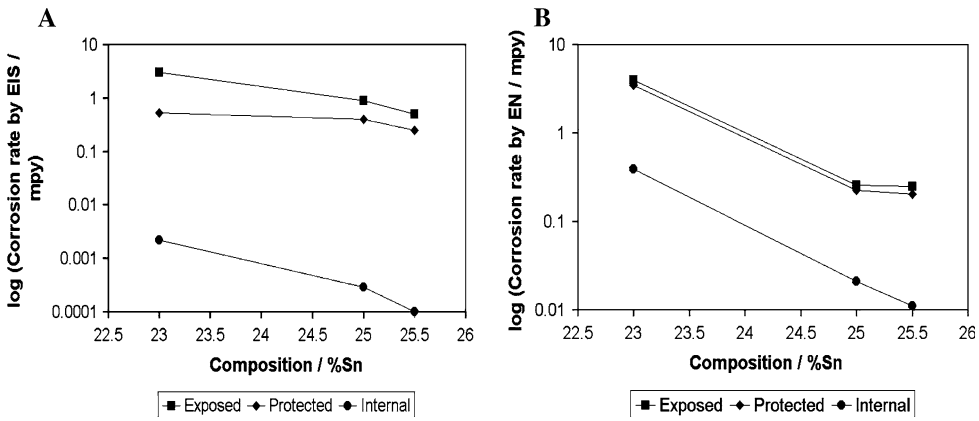

Fig. 16 Corrosion rates obtained by electrochemical impedance (**a**) and electrochemical noise (**b**), as a function of bronze tin content for the exposed, protected and internal bell surfaces

film rupture repassivation transients associated to pitting initiation and propagation events [22]. The highest amplitude transients observed belongs to the internal bell metal surface. The other two present trains of pulses of lower amplitude for exposed and protected bell metal surface. These suggest a more protective passive film and more localized attack present over the internal surface and more porous films over the exposed and protected bell metal surfaces. The noise resistance for overall corrosion increased as a function of time during this experiment. It rose from 5.0 E8 for the bell metal surfaces to 1.0 E10 Ω cm^2 for the cast metal. This is reflected in the impedance noise spectra obtained and presented in Fig. 15.

Figure 16 presents the average corrosion rate (mils per year) obtained for the three bells as function of their tin content. Calculations were made processing the experimental data obtained from the electrochemical impedance and noise measurements using the Stern–Geary equation. The value used for R_p was the R_{ct} value for the impedance technique and the R_n for the noise technique. The results from both techniques show very similar trends. The corrosion rate is a function of tin content diminishing its rate as the tin content becomes higher. Also, the corrosion rate decreases as a function of exposure conditions: exposed > protected > internal.

4 Conclusions

Experimental duplication of the metal core of the bells using same chemical composition and based in historic sources was not possible. Eutectoid structure appeared instead of solid solution found in the bells. This implies that the manufacture process of these artifacts remains an open question. The difference of volume between the modern cast coupons and the bodies of the bells may have a role in the observed results because of differential cooling rates.

The uncracked and most ancient bell showed a different electrochemical behavior suggesting that chemical composition has a direct impact in the durability of this kind of artifacts. The causes of the cracking of the other two bells were attributed as first option to corrosion fatigue because the bells were exposed to nitrogen based pollutants during part of their history. Still, no chemical evidence was found to support this statement.

The contents of lead and tin in the bronze alloys were related to corrosion rates. The open circuit corrosion potential appears to be related to the lead content. As the content of lead increases, the free corrosion potential is more active. Therefore, pitting potential is directly related to the lead content.

The corrosion potential is also directly related to the tin content. As more tin appears in the alloy the corrosion rate decreases. In conservation terms, this means that an historic bell may present more resistance to corrosion as the tin content becomes higher. This information is very useful to establish the intervention priority for a number of historic artifacts.

All materials present passive conditions and the passive potential range appear to be related to the lead content in the alloy. Impedance data suggest the corrosion process under the experimental conditions is mixed controlled by a charge transfer and diffusion process through the protective passive layer.

The main form of attack is localized pitting attack over the passive film, this is especially so for the internal bell surface. The corrosion rate is a function of tin content and exposure conditions.

References

1. Rios Szalay A (1998) World heritage in Mexico. Fondo Editorial de la Plática Mexicana, México

2. Urbani G (1996) In: Price NS, Talley MK Jr, Vaccaro AM (eds) Historical and philosophical issues in the conservation of cultural heritage. The Getty Conservation Institute, USA
3. Gómez Orozco F (1943) Congreso Terciario Franciscano de el "Santo Evangelio" de México, Conferencias Literarias Miguel Dorantes Aguilar. Monografía del Convento e Iglesia Franciscanos de Cuernavaca Morelos, México
4. Veleva L, Quintana P, Ramanauskas R et al (1996) Electrochim Acta 1641:1645
5. Fonseca ITE, Picciochi R, Mendoça MH et al (2004) Corros Sci 547:561
6. Robbiola L, Blengino JM, Fiaud C (1998) Corros Sci 2083:2111
7. Calvo A (1999) Conservación y Restauración. Materiales, técnicas y procedimientos de la A a la Z. Ediciones del Serbal, España
8. Fitzgerald KP, Nairn J, Atrens A (1998) Corros Sci 2029:2050
9. Graedel TE, Nassau K, Franey JP (1987) Corros Sci 639:657
10. Morissette JR (1992) Sauvegarde des monuments de bronze. Ministère des Affaires Culturelles, Canada
11. Carrillo y Gariel A (1989) Campanas de México. Instituto de Investigaciones Estéticas, UNAM, México
12. Morcillo M, Almeida E, Rosales B et al (1998) Corrosión y protección de metales en las atmósferas de Iberoamérica = Corrosão e proteção de metais nas atmosferas da Iberoamerica. CYTED, Madrid
13. Elvers B, Hawkins S, Arpe HJ et al (1993) Ullmann's encyclopedia of industrial chemistry. VCH, Weinheim
14. Uruchurtu-Chavarín J, Malo M (1997) Trends Corros Res 49:58
15. Subramanian PR, Chakrabarti DJ, Laughlin DE (1994) Phase diagram of binary copper alloys. ASM International, USA
16. Mariaca L, Genesca J, Uruchurtu J et al (1999) Corrosividad Atmosférica MICAT-México. Plaza y Valdés, México
17. Krätschmer A, Odnevall Wallinder I, Leygraf C (2002) Corros Sci 425:450
18. Cicileo GP, Crespo MA, Rosales BM (2004) Corros Sci 929:953
19. Scott DA, Swarts Dodd L (2002) J Cult Herit 333:345
20. Squarcialupi MC, Bernardini GP, Faso V et al (2002) J Cult Herit 199:204
21. Perez-Herranz V, Montanes MT, García-Anton J et al (2001) Corrosion 835:842
22. Garcia E, Uruchurtu J, Genesca J (1998) An Quim 335:341